Charged particle production in the Pb+Pb system at 158 GeV/c per nucleon

P. Deines-Jones,[1,*] M. L. Cherry,[1] A. Dabrowska,[2] R. Holynski,[2] D. Kudzia,[2] B. S. Nilsen,[1,†] A. Olszewski,[2]
M. Szarska,[2] A. Trzupek,[2] C. J. Waddington,[3] J. P. Wefel,[1] B. Wilczynska,[2] H. Wilczynski,[2] W. Wolter,[2]
B. Wosiek,[2] and K. Wozniak[2]

[1]*Louisiana State University, Baton Rouge, Louisiana 70803*
[2]*Institute of Nuclear Physics, Krakow, Poland*
[3]*University of Minnesota, Minneapolis, Minnesota 55455*
(Received 23 December 1999; published 20 June 2000)

Charged particle multiplicities from high-multiplicity interactions of 158 GeV/nucleon Pb ions with Pb target nuclei have been measured using high-resolution nuclear emulsion chambers with sensitivity from the peak of the pseudorapidity distribution forward to $\eta > 9$. The characteristics of these interactions have been compared to those of central interactions of 200 GeV/nucleon proton, O, and S beams on silver or bromine targets and to results from simulations using the FRITIOF 7.02 and VENUS 4.12 Monte Carlo event generators. Multiplicities scale with the number of wounded nucleons, although the multiplicities for Pb+Pb interactions in the central region are significantly lower than predicted by either Monte Carlo model. We examine the shape of the pseudorapidity distribution and its dependence on centrality in detail, because in this symmetric system the participant projectile target masses are independent of centrality, so any dependence of the shape on centrality must therefore be a dynamical effect. No dependence of the produced particle pseudorapidity distribution on multiplicity or centrality is seen. VENUS, the only one of the two models which attempts to incorporate reinteraction phenomena, predicts a narrowing of the pseudorapidity distributions for the highest multiplicity events, which we do not observe. In general, FRITIOF produces better fits to the all-charged-particle (primarily pion) data than does VENUS.

PACS number(s): 25.75.−q, 13.60.Le, 25.40.Ve, 29.40.Rg

I. INTRODUCTION

The superposition model of nucleus-nucleus (AA) interactions has been highly successful in describing the general features of particle production in high-energy heavy ion systems. With the availability of beams of ^{208}Pb at the CERN SPS, superposition can now be tested over two orders of magnitude in projectile or target mass from pp to Pb+Pb and three orders of magnitude in the number of nucleon-nucleon (NN) collisions. The Pb+Pb system provides nearly the largest reaction volume achievable and the highest energy densities attainable until RHIC and LHC begin colliding heavy ion beams. In this paper, we report Pb+Pb results from the Krakow-Louisiana-Minnesota (KLM) emulsion chamber exposures (EMU-13) at the SPS. Previous results from EMU-13 and a detailed description of the experiment have been presented in [1,2].

Currently, a major emphasis in this field is the search for nonsuperposition processes in rare events or at high energy densities. In order for a state such as a quark-gluon plasma (QGP) to be produced, superposition must break down via some thermalization process, such as reinteraction. To detect and understand events in which plasma or similar collective behavior occurs, it may well be necessary to have a quantitative understanding of ''ordinary'' superposition and reinteraction physics, especially if events exhibiting collective behavior are rare. The Pb+Pb system is large enough that one might reasonably expect reinteraction to have an observable effect on the distribution of produced particles in the most central events.

At the moment, we lack highly precise predictors of particle production and angular distributions in AA interactions. The simplest and historically the first such predictor is the wounded nucleon model [3], which assumes that the multiplicities n_{AA} scale with the average number of participating or ''wounded'' nucleons W and with the average proton-proton multiplicity n_{pp} at an equivalent energy per nucleon: $n_{AA}(E) = \frac{1}{2}W n_{pp}(E)$. This contrasts with the naive expectation that the multiplicities should scale with the number of NN interactions, which would result in multiplicities much larger than those from the wounded nucleon calculation, since a participating projectile nucleon typically interacts with several target nucleons (~ 5 in central Pb+Pb interactions). At SPS energies, the wounded nucleon model predicts multiplicities which are systematically lower than those observed [4–6], but only by $\sim 15\%$ for all measured systems from pp to Pb+Pb. In fact, the current generation of Monte Carlo codes are no better at predicting multiplicities in ultraheavy systems than the wounded nucleon model, although they do of course provide much more comprehensive predictions of angular distributions, transverse momenta, secondary particle species, etc.

At high energy, individual projectile nucleons should typically interact with several target nucleons before rehadronizing outside the target nucleus. Thus, the physical implication of the relative success of the wounded nucleon model is that interactions of hadronic excitations (''reinteractions'' of the collision products emerging from the initial NN interactions) appear to contribute little to the final-state multiplicity. To look for dynamical effects other than this interesting

but well-known ''wounded nucleon effect'' and to study re-interaction effects in detail, one needs to characterize the multiplicities of AA systems carefully. This paper characterizes the measured Pb+Pb multiplicities and angular distributions and compares them to lighter systems and to predictions from FRITIOF 7.02 [7] and VENUS 4.12 [8]. Other experiments, both electronic [9–13] and emulsion [14–16], have reported measurements of high-energy Pb+Pb interactions, including results on multiplicities, strangeness, and J/ψ production, flow, intermittencies, etc. Measurements made with nuclear emulsions have the unique advantage that their excellent position resolution makes it possible to study the extreme forward direction where the projectile spectators appear [1]. In this study we separate the central region, where effects unique to AA interactions are thought to occur, from the spectator region. Both regions are examined for predicted signs of reinteraction.

In Sec. II we calculate the number of wounded nucleons W. Then in Sec. III we describe the experiment and analysis procedure, and use the measurement of forward charge to demonstrate the validity of the calculation of W. At the same time, we derive a value for the charged particle multiplicity n_0 in the absence of spectators, a value which appears to be lower than expected from the simulations. In the framework of the wounded nucleon model, n_0 is proportional to W. The multiplicity per wounded nucleon m is therefore independent of W and as a result also independent of impact parameter, so that m is an appropriate quantity to test for effects unique to AA collisions. In Sec. IV, we compare the measured value of m for central Pb+Pb collisions to the FRITIOF and VENUS simulation results, to the results of pN interactions at similar energies, and to the results for other AA systems. In Sec. V we look at the detailed shape of the pseudorapidity distributions and find a measured distribution which is broader than predicted by VENUS (either with or without reinteraction) but similar to that predicted by FRITIOF without reinteraction. We then look in the forward region and use the measured shape of the produced particle distribution to separate out the spectators and derive an average transverse momentum for the spectator protons. Since the effects of reinteraction are clearly seen in other experiments looking at produced protons and heavy mesons, for example, our results do not imply that reinteraction is not taking place. They do, however, suggest that the detailed treatment of reinteraction by VENUS is not correct, and that in cases where the total multiplicity and the overall charged particle angular distribution are of interest (for example, in the simulations of high-energy cosmic ray air showers), we find that the predictions of FRITIOF without reinteraction are closer to the measured results than are the values predicted from VENUS with reinteraction.

II. CALCULATION OF THE NUMBER OF PARTICIPANT NUCLEONS

In comparing multiplicities in systems of different sizes, a convenient quantity is the multiplicity per participating nucleon $m = n/W$. In the context of the superposition model, W (the number of wounded nucleons) contains all the geometrical effects, i.e., the effects of nuclear radii, density, and

impact parameter. The other factor m depends only on interaction dynamics.

For inclusive data sets, the number of participants, or wounded nucleons, is given in terms of interaction cross sections σ by [3]

$$W = A_T \frac{\sigma_{NP}}{\sigma_{PT}} + A_P \frac{\sigma_{NT}}{\sigma_{PT}}. \tag{1}$$

Here the subscript P means projectile, T means target, and N denotes an individual nucleon, so that σ_{PT} is the total inelastic hadronic cross section for the projectile nucleus interacting with the target [17–19], and σ_{NP} and σ_{NT} are the corresponding nucleon-nucleus cross sections. The first term in Eq. (1) is the number of wounded target nucleons W_T and the second the number of wounded projectile nucleons W_P. To compute W for central data samples, one uses cross sections which are functions of the maximum impact parameter b_{max} of the sample. The cross sections are computed with a Glauber calculation [20], using the inelastic hadronic cross sections and the nuclear density functions of the target and projectile. The maximum impact parameter of the data sample is derived from the partial cross section for producing events in the sample,

$$\sigma_{part} = \pi b_{max}^2 = \sigma_{PT} \frac{N_{cent}}{N_{tot}}, \tag{2}$$

where N_{cent} is the number of central events in the data sample and N_{tot} is the total number of hadronic AA interactions. N_{tot} is derived either from a minimum bias scan of the emulsions or is calculated from the beam count and the total AA cross section. The Glauber calculation gives the number of participant or ''wounded'' projectile and target nucleons W_P and W_T. One can also calculate the number of target and projectile interactions ν_T and ν_P with the same formalism by assuming that the cross section for nucleons which have been excited by a previous interaction is the same as for unexcited nucleons, σ_{NN}. This assumption is not necessary in the calculation of the number of participants $W = W_T + W_P$, which depends (through σ_{NP}, σ_{NT}, and σ_{PT}) only on σ_{NN} and the nuclear density functions. In this analysis we use numbers of participants and numbers of collisions derived from the FRITIOF simulations [7] of the nuclear collision geometry for the specified maximum impact parameters [Eq. (2)]. The sample of central events discussed here corresponds to impact parameters less than 5 fm, compared to a maximum of $2.4(208)^{1/3} \sim 14$ fm for Pb+Pb. At $b = 5$ fm, the values of W derived from different density functions differ by $\sim 3\%$ or less [21]. The deviation increases for larger impact parameters.

III. EXPERIMENTAL AND ANALYSIS PROCEDURE

The data chosen for this analysis consist of central interactions on targets at least as heavy as the projectile. In these systems, the multiply charged spectator fragments that remain after the interaction provide an indication of the centrality of the collision. The measurements are taken from two

TABLE I. 158 GeV/nucleon Pb+Pb samples.

Sample	Events	$\langle Z_b \rangle$	$\langle n_{prod} \rangle$	$\langle n_{fr} \rangle$	$\langle Q_{\eta \geq 6} \rangle$
$Z_b = 0$	21	0	1400 ± 57	0	50.7 ± 1.8
$Z_b = 2$	25	2	1241 ± 50	1	53.0 ± 1.8
$Z_b = 3 - 6$	24	4.8 ± 0.2	1096 ± 48	2.33 ± 0.10	57.0 ± 1.8
$Z_b = 7 - 12$	32	9.4 ± 0.3	899 ± 39	3.94 ± 0.20	62.8 ± 1.3
$Z_b = 13 - 17$	23	14.5 ± 0.3	779 ± 36	5.96 ± 0.19	67.3 ± 1.6
$Z_b = 18 - 25$	24	21.0 ± 0.5	651 ± 36	7.88 ± 0.31	69.0 ± 1.8
$Z_b > 25$	21	33.2 ± 1.2	468 ± 29	8.67 ± 0.63	71.1 ± 1.6
$n_{prod} \geq 1000$	71	3.2 ± 0.4	1263 ± 43	1.46 ± 0.17	53.3 ± 1.0
Total	170	11.8 ± 0.8	933 ± 38	4.21 ± 0.25	61.5 ± 0.8

different kinds of emulsion experiments. Data from 200 GeV p+Ag/Br [22], O+Ag/Br [23], and S+Ag/Br [23,24] collisions were measured in emulsion stacks, in which the detector was the target, and which consequently had 4π angular acceptance. A sample of 170 events from 158 GeV/nucleon Pb+Pb collisions obtained in CERN experiment EMU-13 was measured in chambers with Pb targets and thin emulsion plates exposed perpendicular to the beam [1]. The Pb chambers were designed specifically so that charge could be measured in a small inclined stack at the downstream end of the chambers [1,2]. In the chambers we measure only the particles in the forward cone, $\theta \leq 0.11$ rad, corresponding to a pseudorapidity $\eta \geq 2.9$. This cone includes the peak of the pseudorapidity distribution. Chambers allow the use of targets other than emulsion, and present less material to induce secondary interactions. In both emulsion chambers and stacks, individual particles can be measured even in the extreme forward region, and the submicron resolution makes it possible to identify the individual tracks of these particles and to measure their individual charges.

In the stacks, heavily ionizing particles (those with ionization greater than 1.4 times minimum) are distinguished from relativistic shower particles, and the numbers of each, N_h and n_s, are recorded. Two selections on the minimum bias sets are made to select central events on heavy targets [5,24]: interactions on the Ag or Br nuclei in emulsion are selected by choosing those events with $N_h > 15$ heavy tracks produced by slow particles from the target, and central events are chosen by selecting those events with no multiply charged beam fragments ($n_{fr} = 0$).

In the analysis of the Pb chambers, no minimum bias scan was performed. Instead, a sample of high-multiplicity events was selected by visually scanning for large events. This scan efficiently detected events with observed charged multiplicities greater than 600 forward of $\eta = 2.9$ (corresponding to total charged multiplicities larger than about 1000 once we account for the angular acceptance) together with an incomplete sample of events with smaller multiplicities [1]. From the measured number of incident primaries and the assumed total hadronic Pb+Pb cross section, $\sigma_{Pb+Pb} = 6.9 \pm 0.5$ b, we estimate that we have measured $(23 \pm 4)\%$ of the hadronic interactions. In 170 events we have fully measured all the particles in the pseudorapidity cone $\eta \geq 2.9$ using an auto-

mated measurement system developed at LSU [25,26]. The measurements of the multiplicities of these events have a systematic uncertainty of 3%.

The charge modules included in the EMU-13 chambers enabled us to make a measurement of the individual charges of the forward emitted projectile fragments either by measuring δ-ray counts or darkness due to the total charged particle ionization [2]. Over all the analyzed events, we observed 540 helium fragments ($Z = 2$) and 175 heavier fragments. The average charge of those fragments with $Z > 2$ is small, 5.3 ± 0.3, as compared to 16.1 ± 0.6 measured in inclusive Pb+Pb interactions [2]. The frequency of projectile fragments with $Z > 2$ is also lower in the selected central collisions, about one fragment per event, while in inclusive interactions we observe on average twice as many such fragments per collision. The measurements of the individual charges of the projectile fragments allow us to define for each analyzed event the quantity $Z_b = \Sigma_{i=1}^{n_{fr}} Z_i$, the total charge bound in multiply charged fragments. This quantity is proportional to the size of the projectile spectator remnant, and therefore is a good measure of the impact parameter of the collision. Details of the chamber measurements and the automatic measurement system are presented elsewhere [1,2,22–26].

The measured multiplicities of the Pb+Pb events must be scaled by an angular acceptance factor to calculate the total produced multiplicities n_{prod}. To determine the acceptance factor, pseudorapidity space is divided into three intervals: $\eta < 2.9$, in which multiplicities are not measured and must be estimated; $2.9 \leq \eta < 6$, in which all events are completely measured, and which is virtually spectator free; and $\eta \geq 6$, which is also measured but which contains spectators as well as produced particles. In the interval $2.9 \leq \eta < 6$, the shapes of the pseudorapidity distributions are independent of the events' overall multiplicity and are reproduced quantitatively by FRITIOF. (See Ref. [1] and Sec. IV.) We therefore use a single acceptance multiplier derived from FRITIOF for events of all multiplicities: $n_{prod}/n_{2.9-6} = 1.80 \pm 0.05$. (We obtain the same multiplier if we use VENUS instead of FRITIOF, even though VENUS produces narrower distributions.) The overall uncertainty in the Pb+Pb estimates of multiplicity, including the 3% measurement uncertainty, is then 4%.

The Pb+Pb data samples used in the analysis are shown in Table I. We tabulate the mean bound charge $\langle Z_b \rangle$, the

TABLE II. Proton-nucleus and nucleus-nucleus central interactions used in the analysis.

System	Event	N_{cent}/N_{tot}	$\langle n_s \rangle$ [a]	b_{max} (fm)	W_P	W_T	ν [b]
$p(200)+$Ag/Br	451	24.4%	22.4 ± 0.4	2.89 ± 0.13	1	4.2 ± 0.1	4.2
$O(200)+$Ag/Br	151	28.4%	172 ± 4	4.3 ± 0.4	14.6 ± 0.4	27.5 ± 1.4	50
$S(200)+$Ag/Br	472	19.8%	288 ± 4	4.0 ± 0.4	28.4 ± 0.8	42.2 ± 2.1	97
$Pb(158)+Pb$	71	9.7%	1263 ± 43 [c]	4.6 ± 0.6	170 ± 7	170 ± 7	767

[a]Errors are statistical, except for Pb+Pb, which includes systematics.

[b]The total number of interactions $\nu = W_T \nu_P = W_P \nu_T$, where, for example, $\nu_T = A_T \sigma_{nn}/\sigma_{nT}$.

[c]Produced multiplicity n_{prod}. See text.

mean singly charged and fragment multiplicities $\langle n_{prod} \rangle$ and $\langle n_{frag} \rangle$, and the forward ($\eta \geq 6$) charge $\langle Q_{\eta \geq 6} \rangle$ for a set of samples selected by different values of Z_b. Note that these event samples are independent. The sample of events with $n_{prod} \geq 1000$ (corresponding to 9.7% of the total interactions) is compared to data from interactions of lighter 200 GeV/nucleon projectiles on silver or bromine (Ag/Br), summarized in Table II, where the average number of intranuclear interactions in the events covers the range from 4.2 for $p+$AgBr to 767 for Pb+Pb.

In the samples of central and semicentral events in Table I, there are only small numbers of spectator protons in the projectile region [1]. Almost all the shower particles in this region are "produced" in the sense that they are either created or are participant protons, which may originate from either incident protons or neutrons. In the stack data sets, heavily ionizing particles are found in the large-angle target region and are excluded from the analysis in order to remove fragments and spectator protons coming from the target spectator. This cut also removes a few produced particles, estimated from VENUS and FRITIOF to be of the order of 2 -3 % of the charged particle multiplicity. Since the Pb+Pb analysis is restricted to the region $\eta \geq 2.9$, heavy target fragments are almost completely excluded from these Pb+Pb data. In both the stacks and the chambers, the centrality selection is made by cutting on the number and charge of beam fragments, which determine Z_b. In the case of the Pb + Pb chamber measurements, however, because the beam and target are of equal size, Z_b is a variable centrality selection which is more sensitive to the centrality than in the other, asymmetric, systems.

The symmetry of the Pb+Pb system, combined with the high multiplicities of these events, allows us to test our Glauber calculations and at the same time look in some more detail at the comparison of measured and calculated multiplicities. In Fig. 1, we plot the total charge contained in the cone $\eta \geq 6$, which includes essentially all of the spectators, against the multiplicity $n_{prod} = 1.80 n_{2.9-6}$ for all the analyzed events. Superimposed on the data above $n_{prod} \geq 1000$ (where the selection is close to 100% efficient) are the averages for samples with different values of Z_b (solid circles), i.e., centrality. The charge intercept of a fit to the Z_b points (upper line) is 79 ± 3, consistent with the charge of the Pb beam, demonstrating that indeed all the spectator charge is contained in the $\eta \geq 6$ cone. For each sample, the calculated spectator charge $82(A-W_P)/A$ (where $A=208$ is the projec-

tile atomic number) has been subtracted from the measured total charge to obtain the average produced multiplicities in the $\eta \geq 6$ cone (large triangles). This charge grows with the multiplicity in a manner consistent with direct proportionality (cf. Sec. IV). This scaling is observed in the Pb+Pb system at lower, spectator-free pseudorapidities than in the p, O, and S+AgBr systems, and is another consequence of the Pb+Pb system's symmetry. This simply means that the shape of this system's pseudorapidity distributions is independent of multiplicity (and centrality). The forward charge data are consistent with the assumption that this behavior also holds in the spectator region. It also suggests that event multiplicity is directly proportional to the number of participants, as expected.

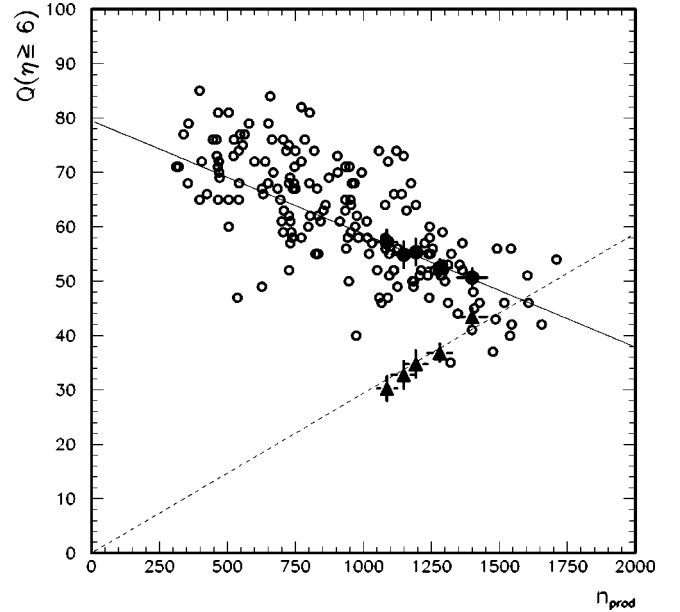The intersection of the two fitted lines at $n_{prod} = 1584$

FIG. 1. Forward charge vs total multiplicity of produced particles (open circles). Large solid circles represent the averages for samples with $n_{prod} \geq 1000$ and $Z_b = 0$, 2, $3-4$, $5-7$, and ≥ 8. Large solid triangles are the calculated produced forward multiplicity $n_{\eta > 6} = Q_{\eta \geq 6} - Q_{spect}$, where Q_{spect} is the spectator charge derived from a Glauber calculation. The upper line is the fit to the data. The intercept is consistent with $Z=82$, the charge of the beam. The lower line is fitted to the forward multiplicity points and is constrained to pass through the origin. The intersection of the two lines is an estimate of the multiplicity in events with no spectators.

TABLE III. Charged multiplicities.

System	m_s	n_{spect}	m_{prod}(data)		m_{prod}(simulations)		m_{pn}
			VENUS	FRITIOF	VENUS	FRITIOF	
p+Ag/Br	4.3 ± 0.1	0	5.5 ± 0.1	4.5 ± 0.1	5.3 ± 0.1	3.9 ± 0.1	3.74 ± 0.03
O+Ag/Br	4.1 ± 0.2	1.0	4.4 ± 0.2	4.2 ± 0.2	4.8 ± 0.1	4.6 ± 0.1	3.74 ± 0.03
S+Ag/Br	4.1 ± 0.1	2.2	4.3 ± 0.1	4.1 ± 0.1	4.8 ± 0.1	4.7 ± 0.1	3.74 ± 0.03
Pb+Pb	3.7 ± 0.2	16.0	3.7 ± 0.2	3.7 ± 0.2	4.7 ± 0.1	4.3 ± 0.1	3.48 ± 0.04

±60 determines the multiplicity[1] of events with no spectator protons n_0. This value agrees with the value determined directly from the $n_{prod}\geq1000$ sample, $2A/W\langle n_{prod}\rangle=1545\pm53$. Thus, the forward charge measurements, the produced particle measurements, and the calculated number of participants together form a tightly consistent picture. If our calculations of the numbers of participants are systematically wrong by as little as $\sim4\%$, our two methods of determining n_0 will no longer agree. Figure 1 therefore indicates that our participant calculations are correct within the stated errors.[2]

The spectator-free multiplicity measured here (1584 ±60) agrees well with the value of 1550 ± 120 determined from the preliminary analysis in [1], and is lower than the value of 1850 expected from the Monte Carlo simulations. We note that results reported by Stenlund *et al.* [14] have also suggested a lower central Pb-Pb multiplicity than expected. We have repeated our analysis by fitting to points chosen on the basis of the number of alphas rather than Z_b, the number of shower particles n_s, and with different radial density distributions, and obtain essentially identical results in all cases. The conclusions that the analysis is self-consistent and that the spectator-free multiplicity is lower than expected appear to be robust.

IV. MULTIPLICITIES PER PARTICIPANT

In order to compare the multiplicities measured with different beam-target combinations, we can use the calculated number of participants to determine the multiplicity per participant for each of our four beam-target systems. Table III shows the average shower particle multiplicities per participant, $m_s=n_s/W$, for the four central data sets of Table II. The first three systems are at 200 GeV/nucleon, and the

Pb+Pb is at 158 GeV/nucleon. In the framework of the wounded nucleon model, the average number of produced particles per participant, $m_{prod}=n_{prod}/W$, is independent of impact parameter. To obtain the quantity n_{prod}, the measured quantity n_s is corrected by subtracting the number of spectator protons and adding the number of produced slow ($\beta<0.7$) particles. The average number of projectile spectator protons, n_{spect}, is estimated from the Glauber calculations. The average number of heavily ionizing slow produced particles is estimated from FRITIOF or VENUS.

Since the FRITIOF and VENUS predictions for the number of slow particles are different, we obtain two values for m_{prod}: one corrected with FRITIOF and one corrected with VENUS. These are listed under m_{prod}(data) in Table III together with the two model predictions under m_{prod}(simulations). The two models give similar results for the heavy ion beams, but because of reinteraction, VENUS predicts a substantially larger multiplicity per participant for the proton beam than does FRITIOF. Both model predictions slightly overestimate the respective measured multiplicities of the O+Ag/Br and S+Ag/Br, and predict significantly too many charged particles in Pb+Pb events. FRITIOF's overprediction of multiplicities in the Pb+Pb system is also discussed in Ref. [1]. However, we note that in the case of Pb + Ag/Br [27], where the target is significantly lighter than the projectile, the total measured multiplicities of high-multiplicity events are consistent with the predictions.

Table III also shows the charged multiplicities per participant, $m_{pn}=n_{pn}^{\pm}/2$, for pn interactions at similar energies [28,29]. We compare to pn data rather than pp data since the pn system is more similar to the AA data in isospin content and charge fraction, both of which affect the NN multiplicities at the 10% level. FRITIOF and VENUS both produce almost equal numbers of protons and neutrons, which is not the case for pp or nn interactions, but is true of pn interactions. In agreement with other studies, we find that the data are systematically higher than predicted [5,6]. Table III appears to indicate that the Pb+Pb value is significantly closer to the wounded nucleon model prediction than are those for the other systems. However, we note that the Pb+Pb system has a significantly different isospin mixture (i.e., a larger neutron excess) than the other systems, which may somewhat reduce its charged multiplicity relative to the other more proton-rich systems. Nevertheless, m_{Pb+Pb} is lower than predicted by both Monte Carlo simulations and empirical extrapolations from lighter systems [4,30].

Figure 2 displays the shower multiplicity densities as a function of pseudorapidity. For each system, the densities

---

[1]Head-on Pb+Pb events have on average about nine spectator protons, and therefore have slightly lower multiplicities than zero-spectator events.

[2]This conclusion depends on the assumption that produced multiplicity can really be plotted as a straight line through the origin as in Fig. 1. Although plausible, this assumption should be tested by extending the data points in Fig. 1 to the left (i.e., to more peripheral events). Our scanning procedure, which was not fully efficient for detecting events with multiplicities smaller than 1000, makes this test impossible. Nevertheless, the good fit of the triangles in Fig. 1 with a straight line through the origin strongly suggests that this assumption is reasonable. The linearity assumption (as suggested by the wounded nucleon model) is discussed and justified further in Sec. V.
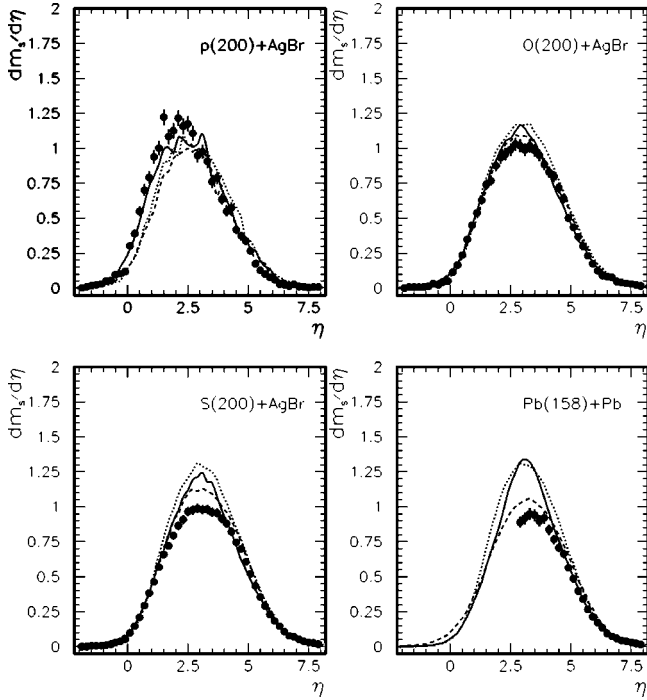
FIG. 2. Densities of shower particles per wounded nucleon, $dm_s/d\eta$, as a function of the pseudorapidity η. The error bars include statistical counting uncertainties in W. For each particular system, the same values of W are used to normalize the data, FRITIOF (dashed lines) and VENUS. VENUS predictions are shown with (solid lines) and without (dotted lines) reinteraction.

have been normalized by the calculated number of wounded nucleons for the data sample. The same normalizations are used for the data and the models. The error bars include uncertainties due to finite counting statistics and uncertainties in the systems' b_{max} (which propagates into the uncertainty in W), added in quadrature. The most obvious conclusion from this figure is that the Pb+Pb system has a significantly lower measured peak density than predicted by either model. Qualitatively, this appears consistent with the trend from lighter to heavier systems. The models slightly underestimate the $p+$Ag/Br central region, overestimate the O+Ag/Br and S+Ag/Br peaks, and significantly overestimate Pb+Pb. FRITIOF provides the better fit in every case.

We have examined the effects of reinteraction predicted by VENUS with separate runs in which reinteraction has been turned off, without adjusting any other parameters in the model. These runs are represented in Fig. 2 by the dotted lines. As expected, reinteraction improves the $p+$Ag/Br fit in the target region [31]. However, turning reinteraction off does not improve the fit to the AA data at midrapidities. This result is discussed in more detail in the next section.

The hypothesis of limiting fragmentation [32,33] states that in hadronic interactions, the density in the target region is asymptotically independent of beam energy and projectile species. When the projectile region is measured in the target rest frame, it is shifted by a kinematically determined amount y_{beam}, but the projectile region densities are otherwise predicted to be independent of energy and target species. This approximate invariance has been observed in pp,
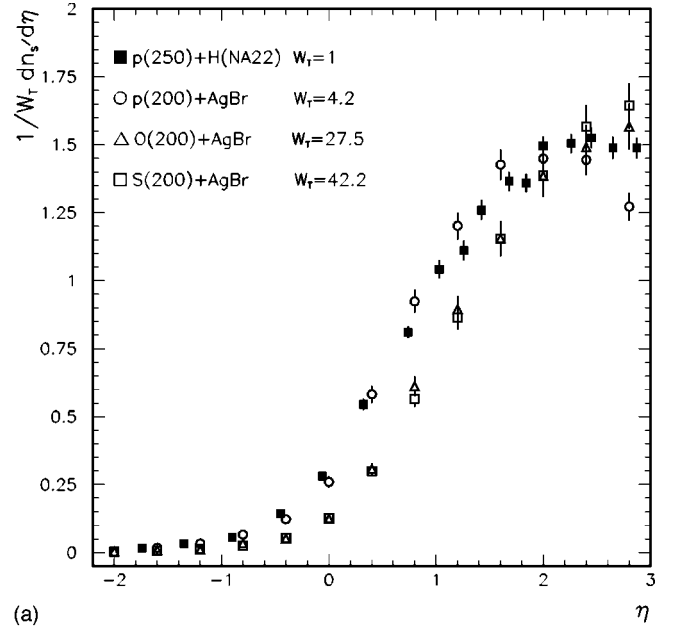
(a)
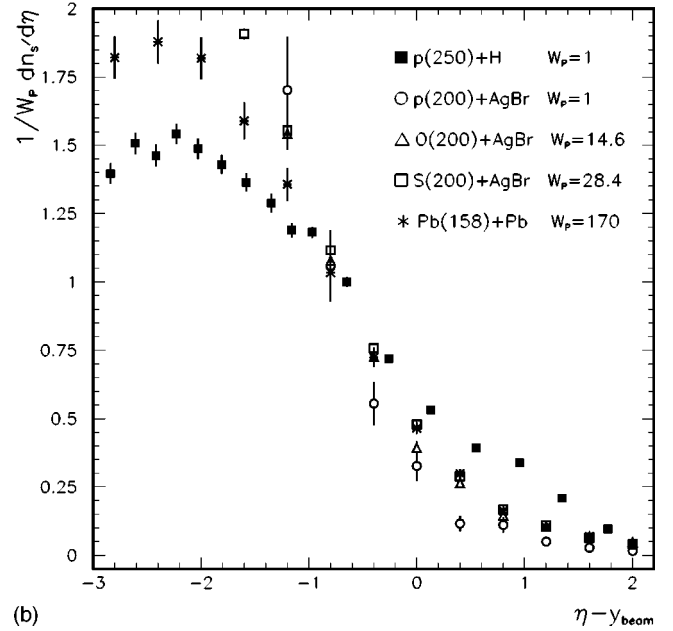
(b)

FIG. 3. Scaling of target and projectile regions with the number of target and projectile participants. Note that the two vertical axes are different. The target region (a) is normalized by W_T, while the projectile region (b) is normalized by W_P.

$\bar{p}p$, pA, and π-emulsion interactions [34–37]. The natural combination of this hypothesis with the principle of incoherent superposition in AA collisions implies that the target region scales with the number of wounded target nucleons W_T and that the projectile region scales with the number of wounded projectile nucleons W_P [38]. This expectation is tested in Fig. 3, which shows the shower densities per wounded target nucleon in Fig. 3(a) and the densities per wounded projectile nucleon in Fig. 3(b). Proton-hydrogen data from the NA22 bubble chamber experiment [39] are shown for comparison to the emulsion data. Figure 3 dem-
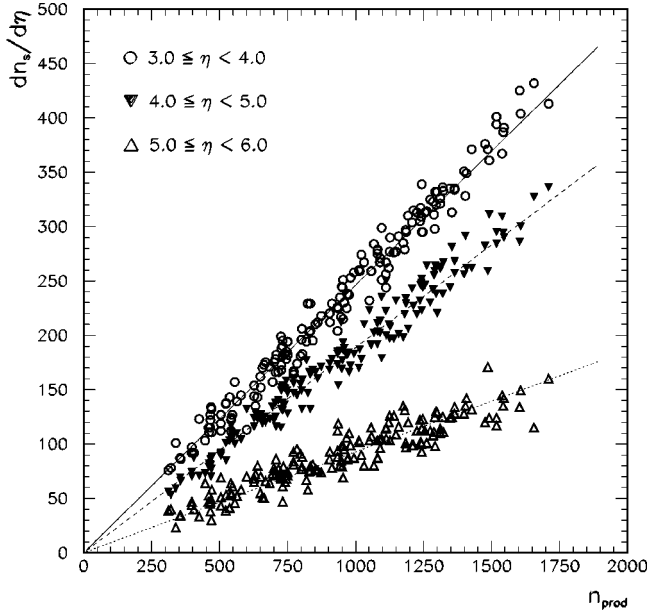
FIG. 4. Dependence of pseudorapidity density with multiplicity in three pseudorapidity intervals. The fitted lines are constrained to pass through the origin.
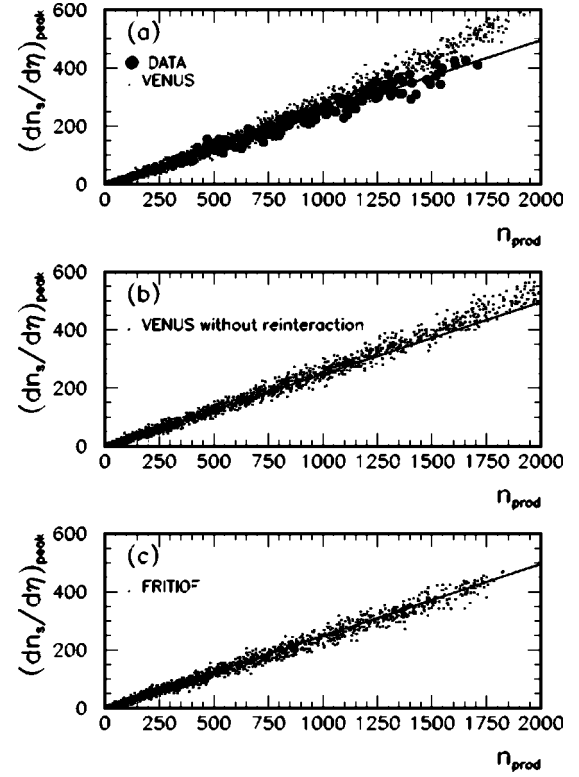

FIG. 5. Comparison of measured peak pseudorapidity densities ($2.9 \leq \eta < 3.6$) with VENUS predictions (a) with reinteraction included and (b) with reinteraction turned off but with all other parameters left unchanged. The comparison with FRITIOF (which does not include reinteraction) is shown in (c).

onstrates that wounded nucleon scaling is a good approximation only for AA systems. There appear to be some deviations from this scaling for pp and pA collisions, but these differences must be interpreted cautiously. First, energy degradation of the projectile passing through the target is significantly different for pp, pA, and AA interactions. In addition, there are different spectator contributions. The bubble chamber acceptance corrections are highest in the projectile region, and the acceptances for slow particles in the target region differ between the two techniques. The $p+$Ag/Br data are lower than the O, S, and Pb data in the projectile fragmentation region, but the excesses in the AA systems are consistent with the calculated number of spectator protons in these systems. There are no projectile spectators in p $+$Ag/Br interactions. The difference between the $p+$Ag/Br data and the AA systems in the target regions appears to be real, and may be due to reinteraction. Nevertheless, over a range of nearly two orders of magnitude in W and $dn/d\eta$, the variation in $(1/W)dn/d\eta$ is only ~ 0.3. The pseudorapidity densities are parametrized quite well with just W_T and W_P, and dynamical effects apparently have only a minor effect on the angular distributions in AA systems in this energy range.

In conclusion, multiplicities in the Pb+Pb system are lower than predicted either by FRITIOF or VENUS, although FRITIOF does significantly better than VENUS. The discrepancy is primarily in the central region. The distributions in the spectator regions appear to be reasonably well understood as the result of fragmentation of W_P or W_T wounded nucleons. We observe no other dynamical effects in the spectator regions except in the $p+$Ag/Br system, where we may be observing the effects of reinteraction in the target region.

V. SHAPES OF Pb+Pb PSEUDORAPIDITY DISTRIBUTIONS

In the Pb+Pb system, the shapes of the shower pseudorapidity density distributions are independent of multiplicity over most of the observed region of pseudorapidity space. This behavior is illustrated in Fig. 4 using the full Pb+Pb data set. The forward region ($\eta \gtrsim 6$) is the sole exception to this rule due to the presence of spectator protons, especially in the more peripheral (lower multiplicity) events, as seen in Fig. 1. Thus, the data in the forward region are consistent with a linear two-component model in which the produced multiplicity is directly proportional to multiplicity (as in Fig. 4) while the spectator contribution decreases linearly with multiplicity from the most peripheral events to the most central ones (Fig. 1). These linearities are predicted by FRITIOF, and are a consequence of superposition in symmetric systems. They hold as long as second-order effects, i.e., reinteraction, are unimportant to the shapes of the pseudorapidity distributions.

VENUS models particle reinteraction, providing an expectation for the influence of reinteraction on the pseudorapidity distributions. Figure 5 relates the peak pseudorapidity density $(dn_s/d\eta)_{peak}$ of the Pb+Pb events to their total produced multiplicity n_{prod}. The straight line shows a linear fit to the data: the data are consistent with direct proportionality between $(dn_s/d\eta)_{peak}$ and n_{prod}. The VENUS-simulated

events, superimposed on the data in Fig. 5(a), deviate from linearity and differ significantly in shape from the data at high multiplicity. This deviation can also be seen in Fig. 2, where VENUS predicts a narrower and taller distribution for central events than is observed. In Fig. 5(b), the data points are suppressed for clarity, but the same straight line fit as in Fig.5(a) is compared to VENUS with reinteraction turned off, but otherwise run with the same parameters. VENUS is more consistent with the data when reinteraction is turned off, although at high multiplicities VENUS still predicts too high a central peak. (For the case of central Pb+Ag/Br collisions as well, a wider distribution than expected from VENUS was observed [27,40].) The best fit to the shape of the distribution is shown in Fig. 5(c), where the FRITIOF predictions are shown to be completely consistent with the linear fit to the data. We should emphasize again that these results do not in any way suggest that reinteraction is not taking place. Other experiments have clearly shown, for example, that the produced protons and kaons are significantly shifted toward midrapidity, a clear sign that these particles are interacting and losing energy [11]. Our results do suggest, however, that the details of the VENUS treatment of reinteraction are not completely correct, and in the case in which only the total multiplicity and angular distribution of all charged particles are of interest, the FRITIOF predictions are in fact closer to the measured values than are the VENUS calculations.

The data are therefore consistent with two conclusions: (1) the shape of the produced particle multiplicity in the spectator region is independent of multiplicity, as it is from $\eta=2.9$ to $\eta=6$, and (2) the shape of the spectator proton distribution is independent of multiplicity. If these conclusions are correct, then we can statistically separate the produced and spectator distributions. Let us define $f_{prod}(\eta)$ and $f_{spect}(\eta)$ to be the normalized produced particle and spectator proton distributions, respectively. We normalize $f_{prod}(\eta)$ to integrate to one in the interval 2.9–5.5, a region which excludes essentially all spectators, and normalize $f_{spect}(\eta)$ such that it integrates to one over $\eta \geqslant 6$. Then the average pseudorapidity distribution $\rho_{samp}(\eta)$ of a sample of events is

$$\rho_{samp}(\eta) = a_{samp} f_{prod}(\eta) + b_{samp} f_{spect}(\eta), \qquad (3)$$

where b_{samp} is the number of spectator protons per event in the sample, and a_{samp} is related to the produced multiplicity through the fraction of particles produced in the interval $\eta=2.9-5.5$: i.e., $a_{samp}=0.52n_{prod}$. If we measure the distributions of a central and a semicentral sample, $\rho_{cent}(\eta)$ and $\rho_{semi}(\eta)$, we can infer the shapes of the produced and spectator proton distributions. For example,

$$f_{spect}(\eta) = \frac{a_{semi}\rho_{cent}(\eta) - a_{cent}\rho_{semi}(\eta)}{a_{semi}b_{cent} - a_{cent}b_{semi}}. \qquad (4)$$

Note that only a_{semi} and a_{cent} affect the shape of the resulting distribution; the numbers of spectators in the two samples b_{semi} and b_{cent} enter only into its normalization.

Our central sample for this analysis is the $Z_b \leqslant 4$ sample. The semicentral sample consists of those events with Z_b
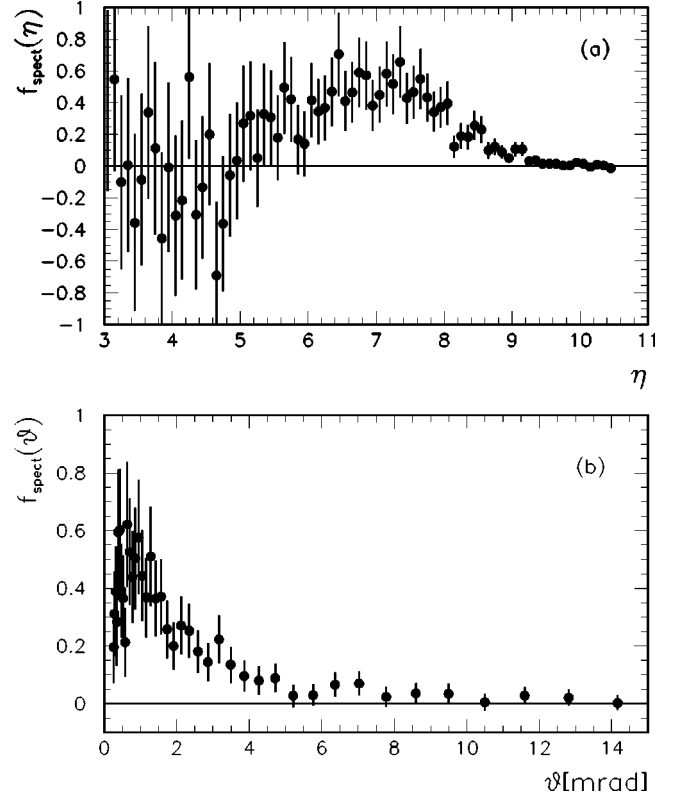

FIG. 6. Derived spectator proton distribution in the Pb+Pb system. The error bars shown are statistical. (a) shows the distribution as a function of pseudorapidity η derived from Eq. (4). (b) shows the distribution transformed into angular units. In (b), the $\eta>9$ data, which have large relative uncertainties in the angle, are not plotted or used in the fit.

>4. The a coefficients are simply the areas under the samples' measured distribution between $\eta=2.9$ and $\eta=5.5$. The b coefficients are evaluated using Fig. 1, which relates the mean multiplicity of each sample to its mean spectator charge Q_{spect} in the $\eta \geqslant 6$ cone. Subtracting the bound charge Z_b gives us an estimate of the number of spectator protons in each sample, which is the same as b_{samp}.

Figure 6(a) shows the resulting spectator distribution $f_{spect}(\eta)$. Figure 6(b) shows the same distribution as a function of θ rather than η. The θ distribution can be fitted to a Gaussian with a half-width of 1.82 ± 0.39 mrad ($\chi^2=0.6$). For spectators having the same longitudinal momentum as the beam, this width corresponds to an rms transverse momentum of (290 ± 60) MeV/c.[3] This is significantly larger than would be expected from an isotropic evaporation model
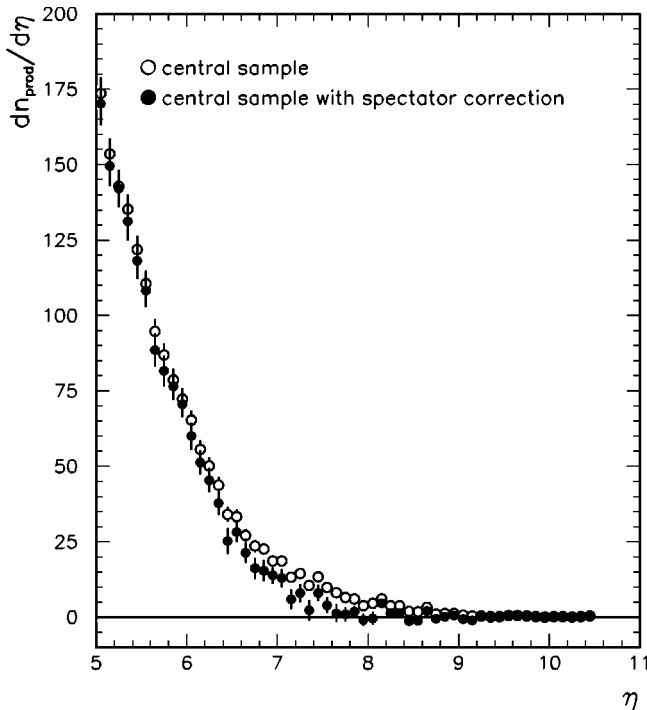

FIG. 7. Comparison of the derived produced particle distribution as a function of pseudorapidity η with the central ($Z_b \leq 4$) sample in the spectator region.

(140 MeV/c). We can also fit the observed distribution to a sum of a Gaussian with a width of 140 MeV/c plus a second Gaussian peaked at $\theta \sim 3$ mrad, corresponding to $p_t \sim 470$ MeV/c. In either case, there is evidence for a wider distribution than expected. Thus, the spectator distribution suggests that there is a rescattered component. This rescattered component, however, is small; the contribution of the second Gaussian to the total is no more than $\sim 20\%$ of the total.

The derived spectator distribution has a small tail extending beyond $\eta = 6$ ($\theta \sim 5$ mrad), indicating that the spectator charge residing outside the $\eta \geq 6$ cone is very small, in agreement with the charge intercept in Fig. 1. The derived produced particle distribution has almost the same shape as that of the central sample, but has a slightly smaller tail, as expected (Fig. 7). We note that the spectator correction improves the agreement between the Pb+Pb and the p+Ag/Br projectile regions in Fig. 3.

In summary, the data are consistent with the shape of $dn_{prod}/d\eta$ being independent of multiplicity over the entire range of pseudorapidity. This independence is directly observed in the central region, where there is no spectator contribution. This result is unexpected in light of the VENUS simulations, and appears to indicate that reinteraction has little influence on the produced particle distribution. On the other hand, the typical p_t values derived for spectator protons are between typical Fermi momenta (~ 100 MeV/c) and proton rescattering p_t values (~ 450 MeV/c), suggesting that reinteraction does play a role in scattering or heating the residual spectators.

VI. DISCUSSION AND CONCLUSIONS

Among high-energy heavy ion systems studied to date, the 158 GeV/nucleon Pb+Pb system is unique in its combination of symmetry with large multiplicities and, consequently, high track statistics in individual events. We have exploited both of these properties in studying centrality criteria, forward multiplicities, and shape-multiplicity dependence. Because of the symmetry of the Pb+Pb system, any shape changes in the pseudorapidity distributions must be due to reinteraction or the onset of nonsuperposition effects, rather than changes in collision geometry. However, we find no evidence for shape changes. Our analyses by no means rule out the occurrence of reinteraction, but taken together, they place stringent limits on rescattering effects in the Pb+Pb system as they might appear in multiplicity or pseudorapidity density measurements. Our study of forward multiplicities of individual events gives us confidence in our participant estimates, and also allows us to plausibly extract information on the transverse momenta of spectator protons. These features of the dataset are summarized in Fig. 1, which brings together the relationships between the multiplicities of central events, forward charge, number of participants, and beam charge.

Perhaps the most interesting finding presented here is the independence of the pseudorapidity shape and the centrality of the collision. This apparently implies that at SPS energies, particle production in the center of mass is not significantly more isotropic in central events than it is in peripheral ones, even in ultraheavy systems. This contrasts with the results from the AGS at 14.6 GeV/nucleon, where pseudorapidity densities from heavy ion interactions become roughly isotropic at the highest multiplicities [41]. Near 200 GeV/nucleon, this anisotropy holds not only in the central region but also in the spectator regions, where we observe scaling with the number of participating projectile or target nucleons: the initial geometry of the system is reflected in the final state.

The fact that rescattering-induced narrowing is predicted to occur but is not observed is puzzling in light of evidence for rescattering from other experiments [9,11,42–44]. In particular, Alber *et al.* [11] compare the NA49 forward veto calorimeter spectra and transverse energy spectra to VENUS and find excellent agreement. We note, however, that a comparison of VENUS with the forward ($\eta \geq 5.9$) and transverse ($2.1 < \eta < 3.4$) energy spectra is very different from a comparison with the detailed pseudorapidity distributions as in Figs. 2 and 5. In VENUS, the narrowing of the distribution with reinteraction occurs because of a combination of greater proton stopping power, slower pions, and enhanced heavy particle production ($\bar{p}p$ pairs and kaons) in the central region. The energy for additional heavy particle production comes in part from increased nucleon slowing and also a slight reduction in pion production. The absence of narrowing in central events may indicate that the degree of slowing of protons and pions in Pb+Pb events is less than the VENUS model predicts. NA44 [9] has in fact shown evidence for a smaller than predicted rapidity shift in the proton rapidity distribution measured for central Pb+Pb collisions. Without the additional energy available for particle production which

comes from increased nucleon stopping power, increased heavy particle production would come at the expense of smaller pion yields. Thus, reinteraction-induced heavy particle production accompanied by a more modest than predicted increase in stopping power could explain both the observed shape independence and the low multiplicities. We note as well that the absence of rescattering in the observed pion distributions is also consistent with the ''sudden hadronization'' picture of Rafelski and Letessier [45] in which the pions are produced directly during the rapid hadronization occurring during the explosion of a dense QGP fireball, with no subsequent equilibration or rescattering.

In conclusion, FRITIOF seems to provide a better simulation of the overall multiplicities and the shape of the charged particle pseudorapidity distribution for these central data than does VENUS. This is particularly noticeable for these very massive Pb+Pb interactions, and becomes less noticeable for the lighter nuclei. The average multiplicities and pseudorapidity distributions in central *AA* interactions on heavy targets at SPS energies are mainly determined by the number of participating nucleons. Multiplicities in these collisions are nonetheless higher than would be expected by simply scaling *NN* multiplicities at the same energy, indicating a dynamical effect at work in addition to the wounded nucleon effect. The dependence of this excess on system mass is not well predicted by the Monte Carlo event generators. The Pb+Pb pseudorapidity distributions appear to have a shape which is independent of multiplicity, placing an important constraint on models of reinteraction in the central region. Indeed, we see no direct evidence for reinteraction in the central region in our all-charged-particle distributions, although it has clearly been seen in other experiments looking, for example, at produced protons and kaons. However, we do find evidence for reinteraction of produced particles or excited matter in the spectators.

ACKNOWLEDGMENTS

[1] P. Deines-Jones *et al.*, Phys. Rev. C **53**, 3044 (1996).

[2] M.L. Cherry *et al.*, Acta Phys. Pol. B **29**, 2155 (1998).

[3] A. Bialas, M. Bleszynski, and W. Czyz, Nucl. Phys. **B111**, 461 (1976).

[4] M.I. Adamovich *et al.*, Z. Phys. C **56**, 509 (1992).

[5] L.M. Barbier *et al.*, Phys. Rev. Lett. **60**, 405 (1988).

[6] S. Fredriksson *et al.*, Phys. Rep. **144**, 187 (1987).

[7] H. Pi, Comput. Phys. Commun. **71**, 173 (1992); L. Ding and E. Stenlund, Lund Report No. LP TP-87-6, 1987.

[8] K. Werner, Z. Phys. C **42**, 85 (1989).

[9] I.G. Bearden *et al.*, Nucl. Phys. **A610**, 175c (1996); I.G. Bearden *et al.*, Phys. Rev. C **58**, 1656 (1998).

[10] F. Antinori *et al.*, Nucl. Phys. **A590**, 139c (1995); E. Anderson *et al.*, *ibid.* **A610**, 165c (1996); I. Kralik *et al.*, *ibid.* **A638**, 115c (1998).

[11] S. Margetis *et al.*, Nucl. Phys. **A590**, 355c (1995); T. Alber *et al.*, Phys. Rev. Lett. **75**, 3814 (1995); S.V. Afanasiev *et al.*, Nucl. Phys. **A610**, 188c (1996); G. Roland *et al.*, *ibid.* **A638**, 91c (1998); H. Appelshäuser *et al.*, Phys. Rev. Lett. (to be published).

[12] M. Aggarwal *et al.*, Nucl. Phys. **A610**, 200c (1996).

[13] M. Gonin *et al.*, Nucl. Phys. **A610**, 404c (1996); M.C. Abreu *et al.*, *ibid.* **A638**, 261 (1998).

[14] E. Stenlund *et al.*, Nucl. Phys. **A590**, 597c (1995); M.I. Adamovich *et al.*, Phys. Lett. B **407**, 92 (1997).

[15] G. Singh and P.L. Jain, Phys. Rev. C **54**, 3185 (1996).

[16] N.M. Astafyeva *et al.*, in *Intersections Between Particle and Nuclear Physics*, edited by T.W. Donnelly, AIP Conf. Proc. 412 (AIP, Woodbury, NY, 1997), p. 269.

[17] J. Letaw, R. Silberberg, and C.H. Tsao, Astrophys. J., Suppl. Ser. **51**, 271 (1983).

[18] G.D. Westfall *et al.*, Phys. Rev. C **19**, 1309 (1979).

[19] B.S. Nilsen *et al.*, Phys. Rev. C **52**, 3277 (1995).

[20] H. Sumiyoshi, Phys. Lett. **131B**, 241 (1983).

[21] For our Glauber calculations, we use parametrizations in At. Data Nucl. Data Tables **14**, 479 (1974). We have compared these parametrizations to those in Pi [7] (and references therein), and J.W. Negele, Phys. Rev. C **1**, 1260 (1970).

[22] E.V. Anzon *et al.*, Yad. Fiz. **22**, 787 (1975) [Sov. J. Nucl. Phys. **22**, 407 (1975)].

[23] A. Dabrowska *et al.*, Phys. Rev. D **47**, 1751 (1993).

[24] O.E. Pruet, Ph.D. thesis, Louisiana State University, 1990.

[25] P. Deines-Jones *et al.*, Nucl. Instrum. Methods Phys. Res. A **390**, 219 (1997).

[26] P. Deines-Jones, Ph.D. thesis, Louisiana State University, 1997.

[27] A. Dabrowska *et al.*, Nucl. Phys. **A633**, 357 (1998).

[28] M. Gazdzicki and O. Hansen, Nucl. Phys. **A528**, 754 (1991).

[29] Particle Data Group, K. Hikasa *et al.*, Phys. Rev. D **45**, S1 (1992).

[30] M.M. Aggarwal and S.I.A. Garpman, Int. J. Mod. Phys. E **4**, 477 (1995).

[31] K. Werner, Phys. Rep. **232**, 87 (1993).

[32] E. Yen, Phys. Rev. D **10**, 836 (1974).

[33] G.J. Alner, Z. Phys. C **33**, 1 (1986).

[34] A. Breakstone *et al.*, Phys. Lett. **132B**, 458 (1983).

[35] G. Giacomelli, Int. J. Mod. Phys. A **A5**, 223 (1990).

[36] M.L. Cherry *et al.*, Phys. Rev. D **50**, 4272 (1994).

[37] W. Thomi *et al.*, Nucl. Phys. **B26**, 365 (1977).

[38] T.H. Burnett *et al.*, Phys. Rev. Lett. **50**, 2062 (1983).

[39] M. Adamus *et al.*, Z. Phys. C **39**, 311 (1988).

[40] B. Wosiek *et al.*, in *Proceedings of the 25th International Symposium Multiparticle Dynamics*, Stara Lesna (World Scientific, Singapore, 1996), p. 271

[41] J. Barrette *et al.*, Phys. Rev. C **46**, 312 (1992).

[42] W.S. Toothacker *et al.*, Phys. Lett. B **197**, 295 (1987).

[43] R. Albrecht *et al.*, Z. Phys. C **38**, 51 (1988).

[44] J. Bächler *et al.*, Phys. Rev. Lett. **72**, 1419 (1994).

[45] J. Rafelski and J. Letessier, Acta Phys. Pol. B **30**, 3559 (1999); Phys. Rev C. (submitted), nucl-th/9903018.